

# Measuring higher-order interferences with a five-path interferometer

Thomas Kauten\*, Robert Keil, Thomas Kaufmann, Benedikt Pressl, and Gregor Weihs

*Institut für Experimentalphysik, Universität Innsbruck,  
Technikerstraße 25, 6020 Innsbruck, Austria*

\*Thomas.Kauten@uibk.ac.at

Within the established theoretical framework of quantum mechanics, interference always occurs between pairs of trajectories. Higher order interferences with multiple constituents are, however, excluded by Born's rule and can only exist in generalized probabilistic theories. Thus, high-precision experiments searching for such higher order interferences are a powerful method to test the validity of the Born rule and distinguish between quantum mechanics and more general theories. Here, we perform such a test in optical multi-path interferometers. Our results permit to rule out the existence of higher order interference terms to an extent which is more than four orders of magnitude smaller than the expected pairwise interference, refining previous bounds by two orders of magnitudes. This establishes the hitherto tightest constraints on generalized interference theories.

Since arising almost a century ago, quantum mechanics has long become an established paradigm for the description of nature on a submicroscopic scale. It is at the basis of an enormous variety of present and potential future applications, such as quantum communication [1, 2], quantum computation [3–5] and protocols like entanglement swapping [6] or teleportation [7]. Moreover, quantum mechanics is technologically utilized in various domains such as lasers [8], microelectronics [9], electron microscopes [10] and magnetic resonance imaging [11, 12]. However, as every physical theory, quantum mechanics is based on fundamental axioms, which by their very nature cannot be proved theoretically, but only tested against experiments. Moreover, it is still not a complete theory to describe the universe as we do not yet have a quantum theory of gravitation. Eventually, one or the other theory will have to be modified or generalized to achieve unification [13]. By testing their fundamental axioms one may find cues on how such a generalization could look like. Here we focus on an experimental test of one of the axioms of quantum mechanics – Born's rule.

The rule [14] states the probabilistic nature of quantum theory, i.e. that the probability density  $P(\mathbf{r}, t)$  for an observation of a quantum object at a certain time  $t$  and a certain position  $\mathbf{r}$  is given by the absolute square of its wavefunction  $\Psi(\mathbf{r}, t)$ :

$$P(\mathbf{r}, t) = \Psi^*(\mathbf{r}, t)\Psi(\mathbf{r}, t) = |\Psi(\mathbf{r}, t)|^2 \quad (1)$$

As a consequence of Born's rule and quantum superposition, interference can take place even for single particles like single photons. For concreteness, consider an interferometer with multiple non-overlapping paths  $k = A, B, C, \dots$  which superpose in some output port to the final wavefunction  $\Psi = \sum_k \Psi_k$ . Eq. (1) implies:

$$P(\mathbf{r}, t) = \sum_k |\Psi_k(\mathbf{r}, t)|^2 + \sum_{k < l} I_{kl}(\mathbf{r}, t), \quad (2)$$

with pairwise (first-order) interference terms  $I_{kl} \equiv \Psi_k \Psi_l^* + \text{c.c.}$ , depending on the relative phase between the

two paths  $k$  and  $l$ . Thus, Born's rule results in interference terms that always originate from pairings of paths, but forbids the possibility of higher order interferences involving more than two paths at once.

In this vein, one can use the presence or absence of higher-order interferences as an experimental probe of Born's rule. First developed by R.D. Sorkin in the context of a measure theory on spacetime [15] one can define a hierarchy of interference terms. In a three-path interferometer with individually blockable paths  $A, B, C$ , and output probabilities  $P_{ABC}$  for all paths being open,  $P_{AB}$  for only paths  $A$  and  $B$  being open, etc., the second-order interference

$$I_{ABC} \equiv P_{ABC} - P_{AB} - P_{AC} - P_{BC} + P_A + P_B + P_C \quad (3)$$

should be zero, if Born's rule holds. Conversely, a significant deviation from  $I_{ABC} = 0$  would be indicative of the existence of higher-order interferences and contradict the conventional quantum theory.

In an optical experiment it can be assumed that the probability  $P$  is proportional to the rate of detected photons  $p$ . Therefore a directly measurable quantity

$$\epsilon_3 \equiv p_{ABC} - p_{AB} - p_{AC} - p_{BC} + p_A + p_B + p_C - p_0 \quad (4)$$

can be defined [16]. The background term  $p_0$  gives the measured signal when all paths are blocked, accounting for detector dark current/dark counts. For better comparison of the results with the expected behavior, one can introduce the normalized quantity  $\kappa_3 \equiv \frac{\epsilon_3}{\delta_3}$  measuring the ratio of hypothetical second-order interference to the sum of the expected first-order interference,  $\delta_3 \equiv |I_{AB}| + |I_{AC}| + |I_{BC}|$ . For interferometers with more than three paths the higher (third, fourth,...)-order interference terms ( $\kappa_4, \kappa_5, \dots$ ) which of course should also be zero can be defined accordingly.

Different experiments have been realized previously to obtain an upper bound on the modulus of the possible second-order interference term. These experiments were implemented in optics [17–19] as well as via nuclear magnetic resonance (NMR) in molecules [20], all in

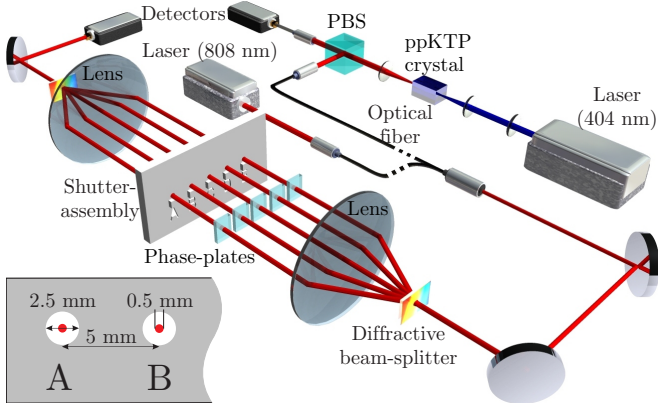


FIG. 1. Experimental setup. The light source is either given by a power stabilized laser or single photons (both at 808 nm) produced via SPDC in a ppKTP crystal pumped by a blue laser. The interferometer consists of two diffractive beam-splitters and two lenses. Shutters and phase plates in each of the paths allow independent manipulation. The inset shows the dimensions and separations of the shutters and the beams.

accordance with the expectation  $\kappa_3 = 0$ . The NMR experiment provided the hitherto tightest constraint with  $\kappa_3 = 0.001 \pm 0.003$ .

As is the case for any such null-test experiment, the tightness of the bound and, thereby, the strength of any conclusions to be drawn about the foundations of the theory depend on the measurement uncertainties. In previous optical three-path interferometers [19], the precision was mostly limited by the phase stability of the interferometer, while the accuracy suffered from detector nonlinearities. In this work, we present a greatly improved multi-path experiment, namely a stabilized five-path interferometer with single photons, with which we are not only able to tighten the bound on second-order interference by two orders of magnitude, but also measure third and fourth-order interference terms in three different regimes: classical, semi-classical and quantum. The five-path interferometer also has the advantage of permitting the acquisition of more statistics for the second- and third-order interference term since it consists of ten three-path interferometers and five four-path interferometers. The systematic error of detector nonlinearities is taken into account by separate detector calibration and a full quantum state tomography of the produced 5-dimensional qudit state.

## RESULTS

A schematic drawing of our setup can be seen in Fig. 1. The measurements were conducted in the classical regime (C) with a coherent laser as source and a photodiode as detector as well as in the semi-classical regime (SC) with unheralded photons from a parametric down

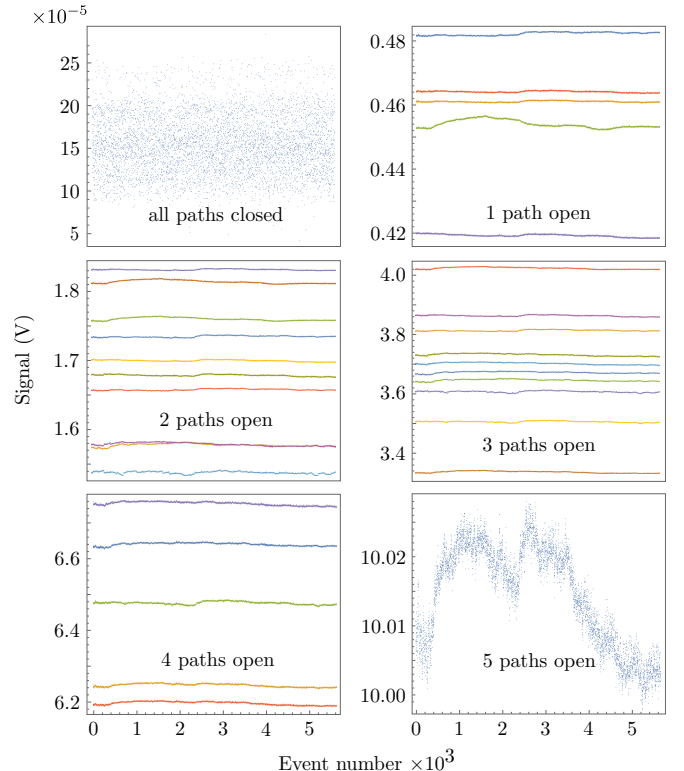


FIG. 2. Measured powers for the different path-combinations with classical light. Each combination is indicated by a separate color within each panel. Extreme outliers have already been removed.

conversion and a single photon detector and in the quantum regime (Q) with heralded single photons. All light sources had a wavelength of 808 nm and were linearly polarized (see Methods). One measurement set consists of the  $2^5 = 32$  different possible open/close combinations of the five paths. Those 32 different combinations were measured in random order to reduce the influence of any memory effects of the detector and of drifts of the source. To achieve good statistics we recorded several thousand measurement sets within a total measurement time of several days. The whole interferometer is shielded against air motion and stray light as well as passively and actively temperature stabilized to a root-mean-square fluctuation  $< 0.02$  K /24 h. Additionally, the phases are actively stabilized by optimizing the phase-plate position after 100 measurement cycles towards maximally constructive interference of all two-path combinations. This point in phase space has been chosen for convenience of alignment and because small phase changes lead only in second order to deviations in output power. This results in a good phase stability over the whole measurement time.

The resulting powers of the different path combinations can be seen in Fig. 2 for the measurement with the power stabilized laser. We filtered the data for ex-

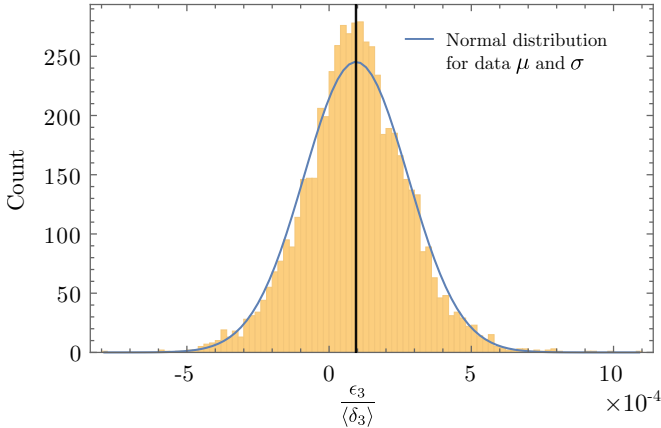


FIG. 3. Histogram of  $\epsilon_3/\langle\delta_3\rangle$  values for an experiment in the classical regime for the three-path subset  $\{A, B, C\}$ . The blue line is a Gaussian fit of the expected distribution of the data and the black bar indicates the mean value with its width being the error (one standard deviation).

treme outliers (resulting from shutter failure) according to Grubbs' test for outliers (with a significance level of 99%) [21, 22]. After that the largest relative standard deviation of all classical signals is 0.3% for 5618 measurement sets recorded within 68 h. For the semi-classical (quantum) single photon measurement with 1912 measurement sets the largest standard deviation was measured to be 3.6% (15.5%) over a measurement time of 88 h. These higher values result mainly from shot noise and from the fact that the power of the blue pump laser was not stabilized.

Due to the anti-correlation between the numerator  $\epsilon$  and the denominator  $\delta$  in the definition of  $\kappa$ , a bias towards positive values can arise from random fluctuations in the data when calculating  $\kappa$  for every shutter cycle and averaging over the data sets. However, calculating the averages of numerator and denominator in the definition of  $\kappa$  separately,

$$\langle\kappa_j\rangle \equiv \frac{\langle\epsilon_j\rangle}{\langle\delta_j\rangle}, \quad j = 3, 4, 5 \quad (5)$$

eliminates their correlations and yields an unbiased estimator of the higher-order interference terms. Indeed, one can show that error sources, which typically occur in interference experiments, such as power fluctuations of the photon source, countrate fluctuations of the detectors (Poissonian photon counting uncertainties), detector/electronic noise, coherent phase fluctuations as well as incoherence, have no systematic effect on the measurement outcome. A detailed discussion on this topic can be found in the Supplementary Material, section S1.

For each of the measured 32-tuples we calculate  $\epsilon_{3,4,5}$  and  $\delta_{3,4,5}$ . A histogram plot of the measured ensemble of  $\epsilon_3/\langle\delta_3\rangle$  in the classical regime is shown in Fig. 3. The other histograms can be found in section S2 in the

Supplementary Material, along with a description of the error analysis of the data. After averaging across all possible path combinations one obtains the mean values and associated uncertainties presented in table I.

	$\langle\kappa_3\rangle$	$\langle\kappa_4\rangle$	$\langle\kappa_5\rangle$
classical ( $\times 10^{-5}$ )	$9.7 \pm 0.1$	$2.7 \pm 0.2$	$0.3 \pm 0.3$
semi-classical ( $\times 10^{-4}$ )	$-9.9 \pm 1.8$	$-5.1 \pm 2.1$	$-3.8 \pm 3.9$
quantum ( $\times 10^{-3}$ )	$-1.1 \pm 1.6$	$0.3 \pm 1.8$	$-2.6 \pm 2.9$

TABLE I. Mean values of the measured higher-order interference terms and their standard errors in the classical (5618 data sets), semi-classical and quantum regime (1912 data sets).

It was recently shown that near-field effects in slit-based measurements can lead to an apparent higher-order interference and, therefore, bias the experiment [23, 24]. However, in our interferometer these effects are of negligible influence, due to the macroscopic separation of the paths (see inset in Fig. 1). Instead, the main systematic uncertainty in our experimental configuration arises from the nonlinearity of the detector. To take this error into account it is useful to fully characterize our five-path interferometer which can be described as a 5-dimensional qudit state. Therefore, we additionally performed a complete quantum state tomography [25, 26]. The density matrix  $\rho$  was numerically reconstructed from a set of single- and two-path measurements with defined phases via a direct reconstruction. We used the direct reconstruction instead a maximum likelihood estimation because it was recently shown that due to the constraint of physicality the maximum likelihood estimation would return a state that deviates systematically from the true state [27] which would bias our results. The real and imaginary parts of the resulting density matrix are shown in Fig. 4. We calculated  $\text{tr } \rho^2 = 0.74$ ; the deviation from 1 (a pure state with no which-path information) can be attributed to an imperfect overlap of the five beams at the second beamsplitter. While this degree of coherence in the interferometer must be determined for an accurate prediction of the influence of the nonlinearities, its actual value has no systematic impact on the Sorkin experiment.

From the density matrix it is possible to calculate the expected powers for the different settings of the shutters in the Sorkin experiment. We found good accordance with our measurement data (see S3 in the Supplementary Material), suggesting that the tomography produces an accurate description of the interferometer. The nonlinearity of both detectors has been characterized in separate experiments [28]. Applying it to the intensities/count rates predicted from the density matrix, yields small corrections of these powers (relative change  $< 0.03\%$  for the laser powers and  $< 0.5\%$  for the unheralded single photon rates).

From these corrected data one can calculate the apparent higher-order interferences  $\kappa_{\text{th}}$ , which one would ex-

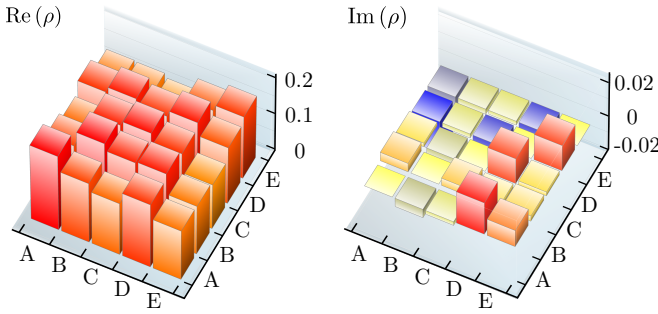


FIG. 4. The density matrix  $\rho$  (reconstructed directly) describes our five-path interferometer via a 5-dimensional qudit state, where  $\text{tr } \rho^2 = 0.74$ .

pect in the Sorkin measurements. The difference between experimentally measured higher-order interferences and the ones expected from nonlinearities  $\tilde{\kappa} \equiv \langle \kappa \rangle - \kappa_{\text{th}}$  gives a corrected higher-order interference as the final result, which can be found in table II.

	$\tilde{\kappa}_3$	$\tilde{\kappa}_4$	$\tilde{\kappa}_5$
classical ( $\times 10^{-5}$ )	$0.0 \pm 3.1$	$4.3 \pm 4.4$	$4.2 \pm 5.1$
semi-classical ( $\times 10^{-4}$ )	$1.3 \pm 1.8$	$-1.6 \pm 2.1$	$-3.8 \pm 4.0$
quantum ( $\times 10^{-3}$ )	$0.0 \pm 1.6$	$0.6 \pm 1.8$	$-2.7 \pm 2.9$

TABLE II.  $\tilde{\kappa} \equiv \langle \kappa \rangle - \kappa_{\text{th}}$  is the corrected higher-order interference for classical, semi-classical and quantum measurements. All these values are within one standard deviation of the expected zero value.

Note that in case of the heralded single photon data, no prediction  $\kappa_{\text{th}}$  has been made, as a more involved nonlinearity model is required. Instead, the experimental data is corrected directly for nonlinearities to produce the final result  $\tilde{\kappa}$ . A detailed discussion of the nonlinearity analysis can be found in the Supplementary Material - Section S4. A final summary of all the different  $\tilde{\kappa}_j$  values is presented in Fig. 5. One finds that all these values are within one standard deviation of the expected zero value.

## DISCUSSION

The optical five-path interferometer presented in this work permitted us to experimentally confine the allowed domain of second order interference to an uncertainty of  $3 \times 10^{-5}$  in the classical light regime. This is two orders of magnitude tighter than the bounds obtained from the most precise experiments in any system to date. The uncertainties in the semi-classical and quantum regime of  $3 \times 10^{-4}$  and  $2 \times 10^{-3}$ , respectively, are also much lower than what has been reported before [16, 19]. This new level of precision has been reached by a range of technical improvements over previous interferometers including power stabilization, phase stabilization and increased throughput as well as a judicious analysis of detector non-

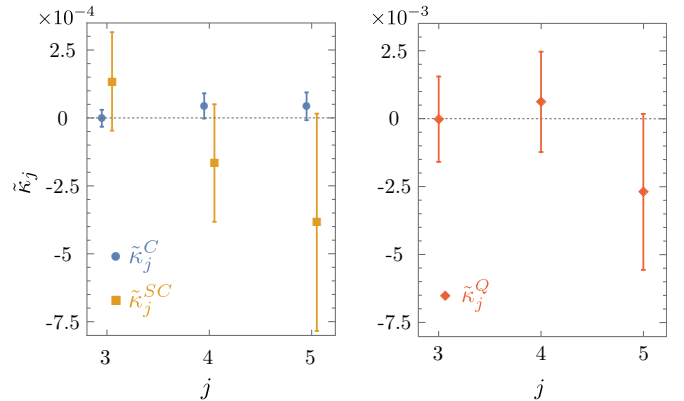


FIG. 5. Final result.  $\tilde{\kappa}$  gives the difference between the experimentally measured  $\langle \kappa \rangle$  and the theoretically predicted  $\kappa_{\text{th}}$  for the measurements in classical (C), semi-classical (SC) and quantum (Q) regime. The order of  $\tilde{\kappa}$  increases along the horizontal axis and the error bars indicate one standard deviation.

linearities, which are the dominant origin of systematic error. Furthermore, we have performed the first measurement of possible third- and fourth-order interference terms, with uncertainties in the same order of magnitude. So far, all our experimental results showed no significant higher-order interferences and are, therefore, in full accordance with the conventional theory. The bounds on higher-order interference determined in our work will be relevant to constrain the allowed parameter space of generalized interference theories, which predict violations of Born's rule [29] or higher-dimensional representations of quantum states [30]. At present, the dominant sources of imprecision in our measurement setup are given by the uncertainties in determining the detector nonlinearities as well as shot noise in the single photon regime. In order to narrow the bound on higher-order interference even more, highly linear detection systems and brighter single photon sources or higher detection efficiency will be required.

## METHODS

### Experimental setup

The coherent laser source is a continuous-wave single frequency laser power-stabilized to 1 mW with relative fluctuations smaller than 0.1% over the complete measurement time of several days by using a liquid crystal noise eater (Thorlabs LCC3112). The single photon source is a 10 mm long periodically poled potassium titanyl phosphate (ppKTP) crystal which is pumped by a blue laser (404 nm), producing photon pairs at 808 nm via type-II spontaneous parametric down conversion. The orthogonally polarized photons are separated on a polarizing beam splitter (PBS). We collect  $6 \times 10^5$  single

photons per second in each of the outputs in single mode fibers and we get  $10^5$  pairs per second at 4 mW pump power. One of the photons serves as a heralding photon, whereas the other is sent through our multi-path interferometer. Therefore we have two possibilities to conduct the measurement with single photons: either free running, where all photons transmitted through the interferometer are counted (yielding a thermal photon number distribution) or conditioned, where only photons are counted if there is a heralding photon (producing a sub-Poissonian distribution) [31]. The interferometer is a Mach-Zehnder type five-path interferometer consisting of a diffractive beam splitter which splits the incoming beam into five almost equally powerful beams, collimated by a lens. A shutter assembly gives the possibility to block or unblock each of the five beams individually, phase plates (glass plates with a thickness of 0.15 mm which are anti-reflection coated for 808 nm) mounted on motorized rotation stages in all of the five beams allow us to set the phase of each path independently. A second lens overlaps the five beams on a second grating at the end of the interferometer before the resulting beam is sent onto a detector. For detecting single photons we used SPCM-AQRH-12-FC single photon counting modules from Perkin Elmer followed by a quTAU time-to-digital converter from qutools GmbH. This system has a deadtime of  $(33.85 \pm 0.31)$  ns and  $(150 \pm 18)$  dark counts per second. As a detector for the laser we employed a Physimetron A139-001 photoreceiver based on a Si-photodiode (Hamamatsu S2386-18K) and a 1 MV/A transimpedance amplifier which was read out by an Agilent 34410A multimeter. This detection system has a low maximum nonlinearity of less than 35 ppm [28].

## ACKNOWLEDGEMENTS

This work was supported in part by the Foundational Questions Institute (FQXi) through Grant No. 2011-02814, the Canadian Institute for Advanced Research (CIFAR) through its Quantum Information Science Program and by the European Research Council (ERC) through project 257531 - EnSeNa. R.K. is supported via a Lise-Meitner-Fellowship of the Austrian Science Fund (FWF) (project M 1849).

## AUTHOR CONTRIBUTIONS

All authors analyzed the data, discussed the results and co-wrote the manuscript.

## ADDITIONAL INFORMATION

Supplementary information is available in the online version of the paper.

## COMPETING FINANCIAL INTEREST

The authors declare that they have no competing financial interests.

---

- [1] Duan, L.-M., Lukin, M. D., Cirac, J. I. & Zoller, P. Long-distance quantum communication with atomic ensembles and linear optics. *Nature* **414**, 413–418 (2001).
- [2] Gisin, N. & Thew, R. Quantum communication. *Nat Photon* **1**, 165–171 (2007).
- [3] Nielsen, M. A. & Chuang, I. L. *Quantum Computation and Quantum Information* (Cambridge University Press, 2000).
- [4] Knill, E., Laflamme, R. & Milburn, G. J. A scheme for efficient quantum computation with linear optics. *Nature* **409**, 46–52 (2001).
- [5] Ladd, T. D. *et al.* Quantum computers. *Nature* **464**, 45–53 (2010).
- [6] Pan, J.-W., Bouwmeester, D., Weinfurter, H. & Zeilinger, A. Experimental entanglement swapping: Entangling photons that never interacted. *Phys. Rev. Lett.* **80**, 3891–3894 (1998).
- [7] Boschi, D., Branca, S., De Martini, F., Hardy, L. & Popescu, S. Experimental realization of teleporting an unknown pure quantum state via dual classical and Einstein-Podolsky-Rosen channels. *Phys. Rev. Lett.* **80**, 1121–1125 (1998).
- [8] Maiman, T. H. Stimulated optical radiation in ruby. *Nature* **187**, 493–494 (1960).
- [9] Mitin, V. V., Kochelap, V. A. & Stroscio, M. A. *Quantum heterostructures: microelectronics and optoelectronics* (Cambridge University Press, 1999).
- [10] Rudenberg, H. G. & Rudenberg, P. G. Chapter 6 - origin and background of the invention of the electron microscope: Commentary and expanded notes on memoir of Reinhold Rüdenberg. In Hawkes, P. W. (ed.) *Advances in Imaging and Electron Physics*, vol. 160, 207 – 286 (Elsevier, 2010).
- [11] Lauterbur, P. C. Image formation by induced local interactions: Examples employing nuclear magnetic resonance. *Nature* **242**, 190–191 (1973).
- [12] Mansfield, P. & Grannell, P. K. NMR 'diffraction' in solids? *Journal of Physics C: Solid State Physics* **6**, L422 (1973).
- [13] Kiefer, C. Why quantum gravity? In Stamatescu, I.-O. & Seiler, E. (eds.) *Lecture Notes in Physics*, vol. 721, 123–130 (Springer Berlin Heidelberg, 2007).
- [14] Born, M. Zur Quantenmechanik der Stoßvorgänge. *Zeitschrift für Physik* **37**, 863–867 (1926).
- [15] Sorkin, R. D. Quantum mechanics as quantum measure theory. *Modern Physics Letters A* **09**, 3119–3127 (1994).

- [16] Sinha, U. *et al.* Testing Born's rule in quantum mechanics with a triple slit experiment. *AIP Conference Proceedings* **1101**, 200–207 (2009).
- [17] Sinha, U., Couteau, C., Jennewein, T., Laflamme, R. & Weihs, G. Ruling out multi-order interference in quantum mechanics. *Science* **329**, 418–421 (2010).
- [18] Hickmann, J. M., Fonseca, E. J. S. & Jesus-Silva, A. J. Born's rule and the interference of photons with orbital angular momentum by a triangular slit. *EPL (Euro-physics Letters)* **96**, 64006 (2011).
- [19] Söllner, I. *et al.* Testing Born's rule in quantum mechanics for three mutually exclusive events. *Foundations of Physics* **42**, 742–751 (2012).
- [20] Park, D. K., Moussa, O. & Laflamme, R. Three path interference using nuclear magnetic resonance: a test of the consistency of Born's rule. *New Journal of Physics* **14**, 113025 (2012).
- [21] Grubbs, F. E. Sample criteria for testing outlying observations. *Ann. Math. Statist.* **21**, 27–58 (1950).
- [22] Grubbs, F. E. Procedures for detecting outlying observations in samples. *Technometrics* **11**, 1–21 (1969).
- [23] De Raedt, H., Michelsen, K. & Hess, K. Analysis of multipath interference in three-slit experiments. *Phys. Rev. A* **85**, 012101 (2012).
- [24] Sawant, R., Samuel, J., Sinha, A., Sinha, S. & Sinha, U. Nonclassical paths in quantum interference experiments. *Phys. Rev. Lett.* **113**, 120406 (2014).
- [25] Thew, R., Nemoto, K., White, A. & Munro, W. Qudit quantum-state tomography. *Phys. Rev. A* **66**, 012303 (2002).
- [26] Altepeter, J., Jeffrey, E. & Kwiat, P. Photonic state tomography. vol. 52 of *Advances In Atomic, Molecular, and Optical Physics*, 105 – 159 (Academic Press, 2005).
- [27] Schwemmer, C., Knips, L., Richard, D., Weinfurter, H. Moroder, T., Kleinmann, M., and Gühne, O. Systematic Errors in Current Quantum State Tomography Tools. *Phys. Rev. Lett.* **114**, 080403 (2015)
- [28] Kauten, T., Pressl, B., Kaufmann, T. & Weihs, G. Measurement and modeling of the nonlinearity of photo-voltaic and Geiger-mode photodiodes. *Review of Scientific Instruments* **85** (2014).
- [29] Trojek, P. *et al.* Experimental multipartner quantum communication complexity employing just one qubit. *Natural Computing* **12**, 19–26 (2013).
- [30] Dakić, B., Paterek, T. & Brukner, Č. Density cubes and higher-order interference theories. *New Journal of Physics* **16**, 023028 (2014).
- [31] Bocquillon, E., Couteau, C., Razavi, M., Laflamme, R. & Weihs, G. Coherence measures for heralded single-photon sources. *Phys. Rev. A* **79**, 035801 (2009).